

# Magnetic Field Geometry in “Red” and “Blue” BL Lacs

P. Kharb ([rhea@iiap.ernet.in](mailto:rhea@iiap.ernet.in))

*Indian Institute of Astrophysics, Bangalore 560 034, India*

D.C. Gabuzda

*Physics Department, University College Cork, Cork, Ireland*

P. Shastri

*Indian Institute of Astrophysics, Bangalore 560 034, India*

**Abstract.** We compare the systematics of the magnetic field geometry in the “red” low-energy peaked BL Lacs (LBLs) and “blue” high-energy peaked BL Lacs (HBLs) using VLBI polarimetric images. The LBLs are primarily “radio-selected” BL Lacs and the HBLs are primarily “X-ray selected”. In contrast to the LBLs, which show predominantly transverse jet magnetic fields, the HBLs show predominantly longitudinal fields. Thus, while the SED peaks of core-dominated quasars, LBLs and HBLs form a sequence of increasing frequency, the magnetic field geometry does not follow an analogous sequence. We briefly investigate possible connections between the observed parsec-scale magnetic field structures and circular polarization measurements in the literature on various spatial scales.

## 1. Introduction

The central regions of Active Galactic Nuclei (AGN) are far more powerful emitters than all the stars of the galaxy combined. AGN classified as BL Lac objects are characterized by a predominantly non-thermal, highly polarized continuum that is variable in both total intensity and polarization at all observed wavelengths, with weak or no optical line emission. All but the last characteristic are shared by Optically Violently Variable (OVV) quasars. These extreme phenomena are understood as a consequence of relativistic beaming in their nuclei.

The near-consensus view of AGN is that they are powered by mass flows around a super-massive black hole. The details of the physical processes are still not well-understood, however, and we do not yet have a comprehensive theory of AGN that can predict the whole range and variety of observed AGN properties from a minimal set of well-defined parameters. Therefore, taxonomy as a substitute for quantification of parameters still plays a major role in the investigation of their physics. For example, radio galaxies are classified into types FR I and II since there are no known physical parameter(s) that can explain the whole range in properties of radio galaxies as a class.



© 2018 Kluwer Academic Publishers. Printed in the Netherlands.

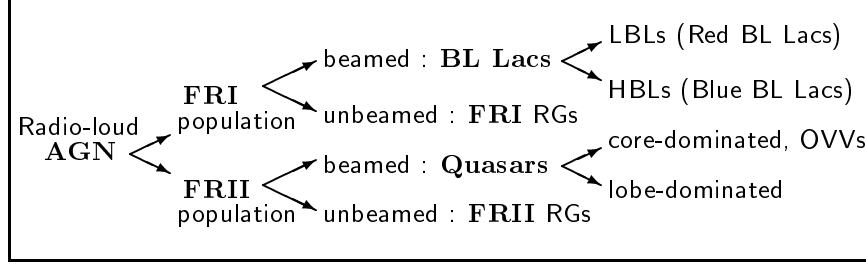


Figure 1. The adopted AGN taxonomy.

In the “radio-loud” AGN (*i.e.*, those AGNs with radio power exceeding the optical power by an order of magnitude or more) there is compelling evidence that bulk relativistic motion (Blandford and Königl, 1979) is ubiquitous, which leads to relativistic aberration effects, so that the angle to the line of sight plays a dominant role in the appearance of these objects (Urry and Padovani, 1995). For every Doppler-boosted object, there are intrinsically similar objects whose jets are not directed toward us – the “parent” population. By comparing properties that are known to be independent of orientation for objects that are known to be boosted and not boosted, we can attempt to identify a given class of Doppler-beamed objects with their plane-of-sky counterparts or “parent objects”. For example, BL Lac objects are believed to be beamed FR I radio galaxies (Orr and Browne, 1982, Wardle et al., 1984), *i.e.*, radio galaxies with relatively low radio luminosities and jets that spread out into diffuse plumes (Fanaroff and Riley, 1974). Similarly, quasars have been identified as beamed FR II radio galaxies (the OVV’s being the most highly beamed ones). This process of identifying beamed and parent objects is known as Unification of AGNs. Whether or not there is a dichotomy in the intrinsic properties of FR I and FR II radio galaxies remains a matter of debate, as is the physical origin of the observed differences.

## 2. “Red” and “Blue” BL Lacs

Among the BL Lacs, two subclasses have emerged. The first BL Lacs were discovered from radio surveys, but X-ray surveys later yielded many more BL Lacs which had somewhat differing properties. The radio-selected BL Lacs (**RBLs**) were typically more core-dominated on arcsec-scales, showed higher average optical polarization and greater variability and had more powerful radio lobes than the X-ray selected BL Lacs (**XBLs**) (Laurent-Muehleisen et al., 1993). In other words, it appeared that the RBLs were more “extreme” than XBLs.

In the light of the fact that orientation is known to play a major role in the observed properties of AGN, it was suggested that RBLs were oriented at closer angles to the line of sight than XBLs – the “Different Angle Scenario” (Stocke et al., 1985). This was explained in the framework of an accelerating jet model (Ghisellini and Maraschi, 1989), wherein the X-rays were radiated in the slower part of the jet and were therefore less beamed than the radio photons coming from the faster portion of the jet. The different-angle scenario predicted that XBLs should be more numerous than RBLs in a statistically complete sample. The prediction was consistent with the observations of the time.

The fly in the ointment was the systematic trend discovered in the spectral energy distributions (**SEDs**) (Figure 2, Urry and Padovani (1995)). The RBL SEDs typically peak in the near infrared (low-energy peaked BL Lacs (**LBLs**) or “red” BL Lacs), whereas the XBL SEDs typically peak in the soft X-ray regime (high-energy peaked BL Lacs (**HBLs**) or “blue” BL Lacs). The different-angle scenario could not explain this difference in the SED peaks. Most, though not all, RBLs are LBLs and most, though not all, XBLs are HBLs. We will adopt this latter terminology, since it is more physical.

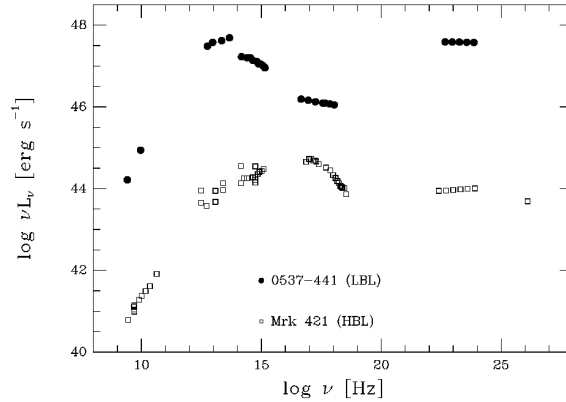


Figure 2. Spectral Energy Distributions show that the synchrotron peaks for the LBLs lie in the NIR/optical regime and for HBLs in the EUV/soft-X-ray regime.

The discovery of the systematic differences in the SED peaks of the “blue” HBLs and “red” LBLs gave rise to the alternative “Different Energy Cutoff Scenario,” wherein the X-ray emitting regions of HBLs have higher electron Lorentz factors or magnetic fields than LBLs (Sambruna et al., 1996). This scenario would then predict that LBLs should be more numerous than HBLs.

### 3. Motivation

The peaks of the SEDs of core-dominated quasars (CDQs), LBLs and HBLs form a sequence of increasing frequency. The CDQs are thought to be beamed FR II radio galaxies, while the BL Lac objects are thought to be beamed FR I radio galaxies. As if reflecting this dichotomy, there is a systematic difference between the magnetic-field geometries observed for the VLBI jets of BL Lacs (mostly LBLs) and CDQs, *viz.*, the ordered component of the jet magnetic field tends to be parallel (perpendicular) to the local jet direction in CDQs (LBLs) (Cawthorne et al., 1993, Gabuzda et al., 2000).

We wished to explore the parsec-scale magnetic field geometries in the HBLs, to see if this geometry reflected the sequence in the SED peaks. We accordingly undertook pc-scale polarimetric imaging of X-ray selected BL Lacs from the HEAO-1 survey.

### 4. Observations

Polarization VLBI observations were made at 5 GHz in February 1993 (using a global array of three European and six US antennas), July 1995 and June 1998 (both using the NRAO <sup>1</sup> Very Large Baseline Array). The sample consisted of 21 northern hemisphere BL Lacs detected in hard X-rays by the *HEAO*-1 survey (Wood et al., 1984) and six BL Lacs from the *ROSAT*-Green Bank (RGB) sample (Laurent-Muehleisen et al., 1997). Calibration, fringe fitting and imaging were done using the Astronomical Image Processing System (AIPS) with the polarization calibration following standard methods (Cotton, 1989). Results for 4 XBLs from this sample have been previously published (Kollgaard et al., 1996).

### 5. Results

The VLBI polarization observations of LBLs (primarily from the 1-Jy sample (Kuehr and Schmidt, 1990), *e.g.*, Gabuzda et al. (2000) and references therein) and HBLs (our work) reveal that both LBLs and HBLs have compact “core-jet” morphologies. We present the radio maps of some of the objects from the HEAO-1 sample in Figures 3–4.

Several of the HBLs that we have observed show evidence for a “spine+sheath” magnetic-field structure, with the inner region of the jet having transverse  $\mathbf{B}$  field and the edges having longitudinal magnetic

---

<sup>1</sup> The National Radio Astronomy Observatory is a facility of the National Science Foundation operated under cooperative agreement by Associated Universities, Inc.

field. This type of  $\mathbf{B}$ -field structure could be a result of interaction of the jet with the surrounding medium. Particularly good examples are the HBLs 1230+253 (Figure 4c) and 1727+502 (Figure 4d). This may point in the direction of a helical magnetic field threading the jets of at least some of these objects, which could have implications for mechanisms for the production of circular polarization in them.

The orientation of the parsec-scale core polarizations of HBLs and LBLs relative to the inner VLBI jet direction do not show any obvious systematic differences. In both cases, there is a clear tendency for the core polarization electric vectors to lie either parallel or perpendicular to the jet direction (Gabuzda et al., 2000). The physical origin of this bimodal behaviour is not entirely clear, though it may be due at least in part to optical depth effects (Gabuzda, these proceedings).

In contrast, the *jet* polarizations of HBLs and LBLs do display systematic differences, as can be seen in Table I. Among both types of BL Lac there are sources in which the observed jet polarization angles lie parallel or perpendicular to the local jet direction. However, the polarization angles are perpendicular to the jet in the majority of HBLs, while they are aligned with the jet in the majority of LBLs. Assuming that the emission region is optically thin, which is certainly the case for the jet, we infer that the magnetic ( $\mathbf{B}$ ) field is perpendicular to the observed polarization angle. Thus, the LBLs show predominantly *transverse* jet magnetic fields, while the HBLs show predominantly *longitudinal* jet fields.

Table I. Systematics of B field geometry in the two subclasses of BL Lacs.

<b>B field structure in the VLBI jet</b>	<b>LBL</b>	<b>HBL</b>
<b>B</b> is transverse to local jet	65 %	35 %
<b>B</b> is parallel to local jet	35 %	55 %
No obvious relation	–	10 %

Since the jets of CDQs exhibit predominately *longitudinal* magnetic fields, we find that the systematics of the jet  $\mathbf{B}$  field geometry in CDQs, LBLs and HBLs, which goes from longitudinal to transverse to longitudinal, does not reflect the sequence in the SED peaks.

## 6. Circular polarization

It has been argued that the sequence in the SED peaks of CDQs, LBLs and HBLs might reflect a sequence in magnetic field strength/Lorentz

factors (Sambruna, 1994). Since the detectability of circular polarization may also be linked to the magnetic field strength and/or geometry and the low-end of the Lorentz factor distribution (if the circular polarization is produced by Faraday conversion of linear polarization), we looked for evidence for a connection between the parsec-scale  $\mathbf{B}$  field geometry and previous detections of circular polarization.

To this end we compiled all previous circular polarization measurements we could find in the literature (see Table II). We found such measurements for a total of 73 quasars and 21 BL Lacs, in addition to 52 galaxies, made on various spatial scales. Of the 21 BL Lacs, 19 are LBLs and only 2 are HBLs. We divided the measurements into three groups on the basis of spatial scale: parsec-scale, kiloparsec-scale ATCA, and kiloparsec-scale single-dish (Table II).

Table II. Circular polarization detection rates in Quasars and BL Lacs.

	Detection rate % (no. observed)		
	Single-dish (4, 5) (kpc-scale)	ATCA (3) (kpc-scale)	VLBI (1, 2) (pc-scale)
<b>Quasars</b>	46 % (52)	67 % (15)	23 % (35)
<b>BL Lacs</b>	27 % (11)	60 % (5)	0 % (12)

References : 1: (Homan and Wardle, 1999), 2: (Homan et al., 2001), 3: (Rayner et al., 2000), 4: (Weiler and de Pater, 1983), 5: (Komesaroff et al., 1984)

The statistics are insufficient to discern differences between the circular-polarization detection rates for LBLs and HBLs, since only 2 HBLs were observed in the circular polarization experiments. There is some evidence from the VLBI measurements (Homan et al., 2001) and single-dish measurements (Weiler and de Pater, 1983; Komesaroff et al., 1984) that the circular-polarization detection rate may be higher for quasars than for BL Lacs. Could this be a consequence of the fact that most of the quasars observed have brighter compact nuclei than the BL Lacs ?

Figure 5 shows the distribution of the total flux density on the *relevant* spatial scales for all the circular polarization observations. The observations are again divided into groups as in Table II (see above). In the case of the single-dish measurements of circular polarization (left-most panels in each row), the distributions are of the total flux density of the *compact* component, *i.e.*, from a VLBI measurement, as given in Weiler and de Pater, 1983. In the case of the ATCA and VLBI measurements (middle and right-most panels), the distributions are of the total intensity measured by ATCA and VLBI, respectively. It is especially clear in the VLBI circular polarization measurements

(last column of histograms) that nearly all of the relatively few BL Lac objects for which circular polarization measurements are available fall at the low end of the flux density range for the observed quasars. However, the situation is not clear, since (i) there is no obvious difference in the detection rates for CDQs and BL Lacs in the ATCA measurements (Rayner et al., 2000), and (ii) the quasars in which circular polarization is detected in the ATCA and single-dish observations have flux densities that fall in the same range as those of BL Lac objects. Further, in the single-dish observations of radio galaxies, circular polarization is detected in compact components with much lower flux densities than the weakest components in BL Lacs in which circular polarization is detected.

If systematic differences in the circular-polarization detection rates (or other properties of the circular polarization) observed in CDQs, LBLs and HBLs could reliably be shown to be present or absent, this could lead to interesting clues to the origin of the circular polarization. Circular polarization observations of well-selected samples, for *eg.*, comparable HBLs and LBLs, are needed to search for relationships between magnetic-field geometry and other properties of the compact radio emission and the circular-polarization detection rate. Well-selected samples might necessitate observations of relatively faint sources, but this is not unrealistic as Figure 5 shows. If established, such relationships could potentially provide useful information about the Lorentz factors and magnetic-field strengths in the jets of different subclasses of BL Lacs and quasars.

A circular polarization analysis of all sources in the 1-Jy sample of northern BL Lac objects (mostly LBLs) defined by Kuehr and Schmidt (1990) is underway (Gabuzda and Vitrischak, in preparation).

## 7. Conclusions

1. The ordered component of the  $\mathbf{B}$  fields in the parsec-scale jets of the “blue” HBLs tend to be parallel to the local jet direction. This contrasts with the tendency for the  $\mathbf{B}$  fields in the parsec-scale jets of the “red” LBLs which are perpendicular to the local jet direction.
2. The systematics of the magnetic field geometry thus do not reflect the sequence in the SED peaks of CDQs, LBLs and HBLs.
3. The VLBI core polarization angles do not show any systematic differences between HBLs and LBLs.

4. Several of the observed HBLs show evidence for a “spine+sheath” magnetic-field structure, with transverse  $\mathbf{B}$  field in the inner region of the jet and longitudinal  $\mathbf{B}$  field at the edges. This may point in the direction of a helical magnetic field threading the jets of these objects, in turn having implications for mechanisms for the production of circular polarization in them.
5. Currently available circular polarization measurements in the literature suggest that quasars may be more likely to show detectable circular polarization than BL Lacs. However, the situation is not clear, since the largest difference in detection rates are found in the VLBI measurements, and the low detection rate for the BL Lac objects in this case may be due to the fact that the observed quasars have on average brighter VLBI cores than the BL Lacs.
6. Given the recent advances in circular polarization measurement techniques on both arcsecond (ATCA) and milliarcsecond (VLBI) scales, which have made detections possible in at least a minority of BL Lacs (and quasars) with relatively faint compact cores, it is beginning to become feasible to obtain circular polarization measurements of well-defined samples on various scales. This would then enable *rigorous* tests of the predictions of various scenarios for the physical differences between different types of object.

### Acknowledgements

We would like to acknowledge the contribution made by Ron Kollgaard and Sally Laurent-Muehleisen in initiating the VLBP project on HEAO-1 BL Lacs, without which this work would not have been possible. P. Shastri is grateful to the conference organisers for support that enabled her to make this presentation, and to the Department of Science & Technology and the Council for Scientific & Industrial Research, Govt. of India, for travel support.

### References

- Blandford, R. D. and A. Königl: 1979, ‘Relativistic jets as compact radio sources’. *Astrophys. J.* **232**, 34–48.
- Cawthorne, T. V., J. F. C. Wardle, D. H. Roberts, and D. C. Gabuzda: 1993, ‘Milliarcsecond Polarization Structure of 24 Objects from the Pearson-Readhead Sample of Bright Extragalactic Radio Sources. II. Discussion’. *Astrophys. J.* **416**, 519–+.



- Cotton, W. D.: 1989, ‘Very Long Baseline Interferometry, Techniques and Applications’. eds. *M. Fellini & R.E. Spencer (Dordrecht :Kluwer)* p. 275.
- Fanaroff, B. L. and J. M. Riley: 1974, ‘The morphology of extragalactic radio sources of high and low luminosity’. *Mon. Not. R. astr. Soc.* **167**, 31P–36P.
- Gabuzda, D. C., A. B. Pushkarev, and T. V. Cawthorne: 2000, ‘Analysis of  $\lambda=6$ cm VLBI polarization observations of a complete sample of northern BL Lacertae objects’. *Mon. Not. R. astr. Soc.* **319**, 1109–1124.
- Ghisellini, G. and L. Maraschi: 1989, ‘Bulk acceleration in relativistic jets and the spectral properties of blazars’. *Astrophys. J.* **340**, 181–189.
- Homan, D. C., J. M. Attridge, and J. F. C. Wardle: 2001, ‘Parsec-Scale Circular Polarization Observations of 40 Blazars’. *Astrophys. J.* **556**, 113–120.
- Homan, D. C. and J. F. C. Wardle: 1999, ‘Detection and Measurement of Parsec-Scale Circular Polarization in Four AGNS’. *Astron. J.* **118**, 1942–1962.
- Kollgaard, R. I., D. C. Gabuzda, and E. D. Feigelson: 1996, ‘Parsec-Scale Radio Structure of Four X-Ray-selected BL Lacertae Objects’. *Astrophys. J.* **460**, 174–+.
- Komesaroff, M. M., J. A. Roberts, D. K. Milne, P. T. Rayner, and D. J. Cooke: 1984, ‘Circular and linear polarization variations of compact radio sources’. *Mon. Not. R. astr. Soc.* **208**, 409–425.
- Kuehr, H. and G. D. Schmidt: 1990, ‘Complete samples of radio-selected BL Lac objects’. *Astron. J.* **99**, 1–6.
- Laurent-Muehleisen, S. A., R. I. Kollgaard, G. A. Moellenbrock, and E. D. Feigelson: 1993, ‘Radio morphology and parent population of X-ray selected BL Lacertae objects’. *Astron. J.* **106**, 875–898.
- Laurent-Muehleisen, S. A., R. I. Kollgaard, P. J. Ryan, E. D. Feigelson, W. Brinkmann, and J. Siebert: 1997, ‘Radio-loud active galaxies in the northern ROSAT All-Sky Survey. I. Radio identifications’. *Astron. Astrophys. Suppl.* **122**, 235–247.
- Orr, M. J. L. and I. W. A. Browne: 1982, ‘Relativistic beaming and quasar statistics’. *Mon. Not. R. astr. Soc.* **200**, 1067–1080.
- Rayner, D. P., R. P. Norris, and R. J. Sault: 2000, ‘Radio circular polarization of active galaxies’. *Mon. Not. R. astr. Soc.* **319**, 484–496.
- Sambruna, R.: 1994, ‘Ph.D. thesis, SISSA, Trieste’.
- Sambruna, R. M., L. Maraschi, and C. M. Urry: 1996, ‘On the Spectral Energy Distributions of Blazars’. *Astrophys. J.* **463**, 444–+.
- Stocke, J. T., J. Liebert, G. Schmidt, I. M. Gioia, T. Maccacaro, R. E. Schild, D. Maccagni, and H. C. Arp: 1985, ‘Optical and radio properties of X-ray selected BL Lacertae objects’. *Astrophys. J.* **298**, 619–629.
- Urry, C. M. and P. Padovani: 1995, ‘Unified Schemes for Radio-Loud Active Galactic Nuclei’. *Publ. Astr. Soc. Pacific.* **107**, 803–+.
- Wardle, J. F. C., R. L. Moore, and J. R. P. Angel: 1984, ‘The radio morphology of blazars and relationships to optical polarization and to normal radio galaxies’. *Astrophys. J.* **279**, 93–98.
- Weiler, K. W. and I. de Pater: 1983, ‘A catalog of high accuracy circular polarization measurements’. *Astrophys. J. Suppl.* **52**, 293–327.
- Wood, K. S., J. F. Meekins, D. J. Yentis, H. W. Smathers, D. P. McNutt, R. D. Bleach, H. Friedman, E. T. Byram, T. A. Chubb, and M. Meidav: 1984, ‘The HEAO A-1 X-ray source catalog’. *Astrophys. J. Suppl.* **56**, 507–649.

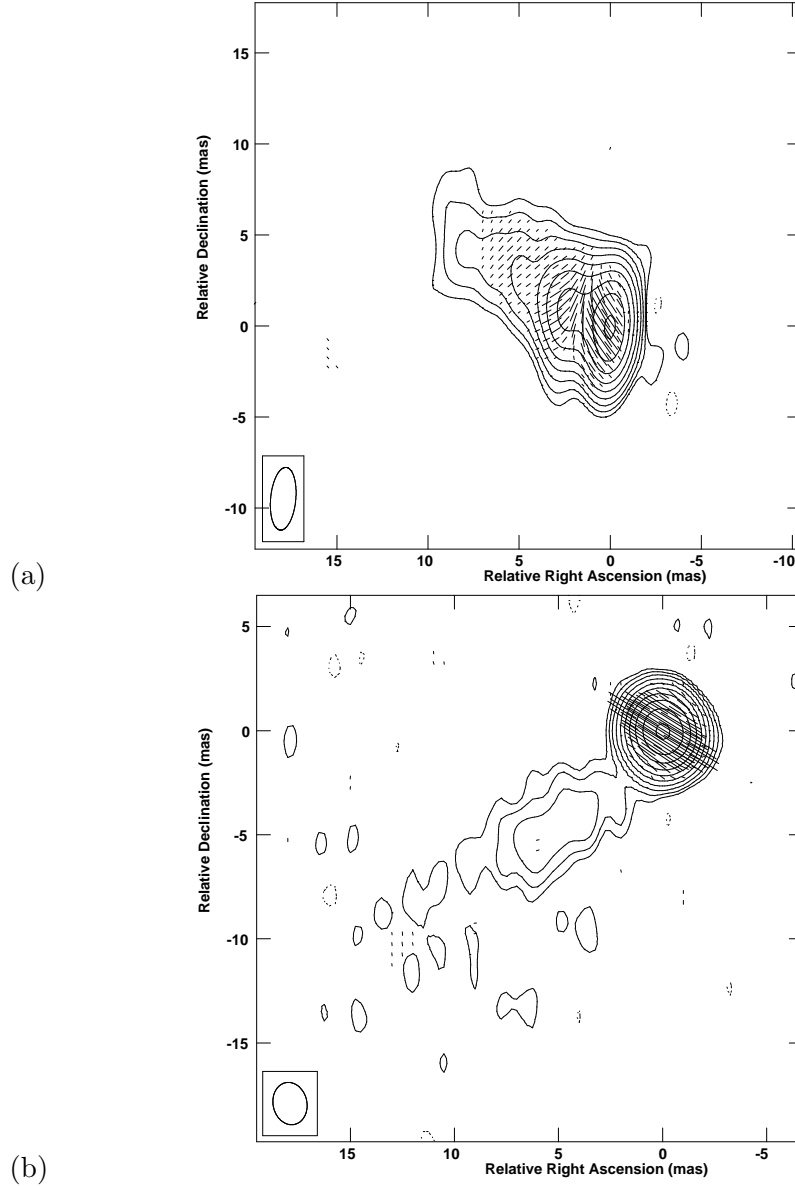


Figure 3. Total intensity VLBI maps of LBLs (a) 0829+046 and (b) 0929+502 at 5 GHz with polarization electric vectors superimposed. Contours are (a) -0.35, 0.35, 0.70, 1.40, 2.80, 5.60, 11.20, 22.50, 45 and 90 per cent of the peak brightness of 441 mJy beam<sup>-1</sup>,  $\chi$  vectors: 1 mas = 8 mJy beam<sup>-1</sup> and (b) -0.17, 0.17, 0.35, 0.70, 1.40, 2.80, 5.60, 11.20, 22.50, 45 and 90 per cent of the peak brightness of 433 mJy beam<sup>-1</sup>,  $\chi$  vectors: 1 mas = 10 mJy beam<sup>-1</sup>.

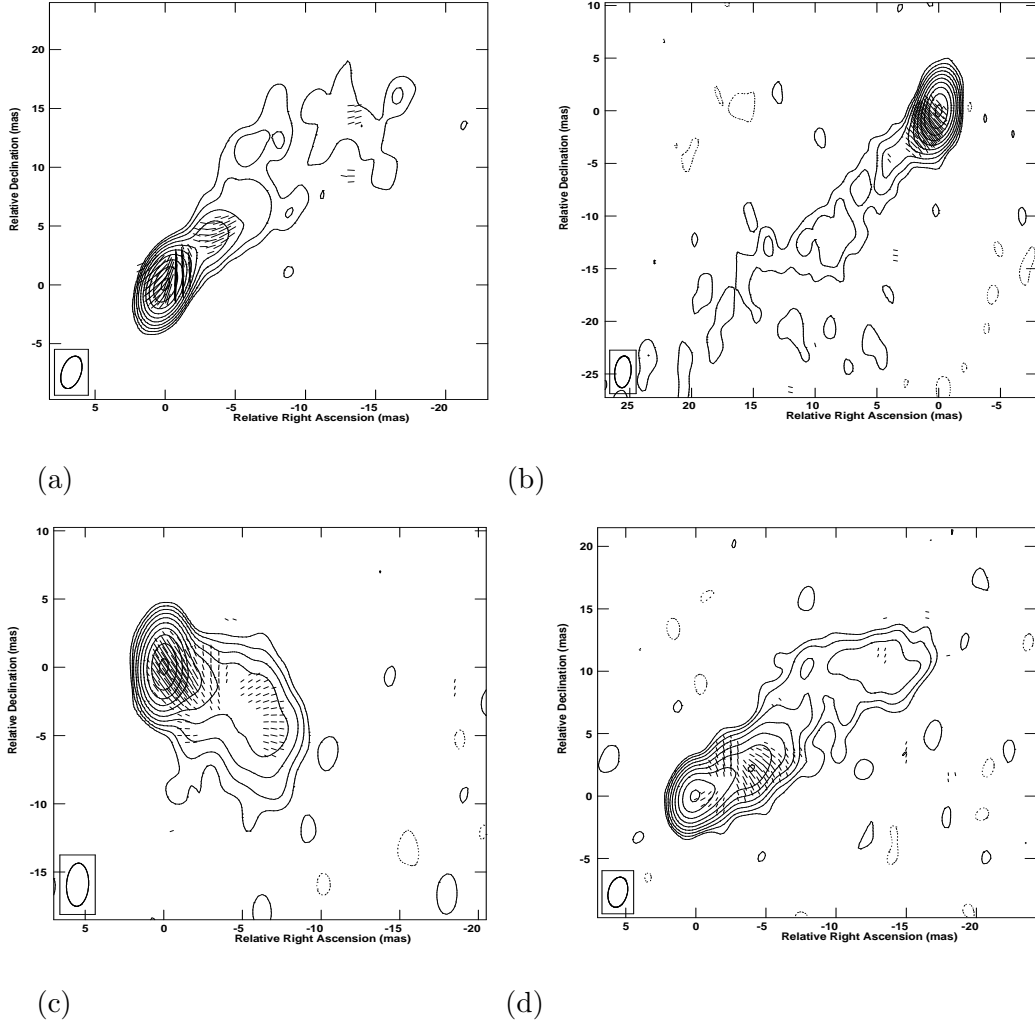
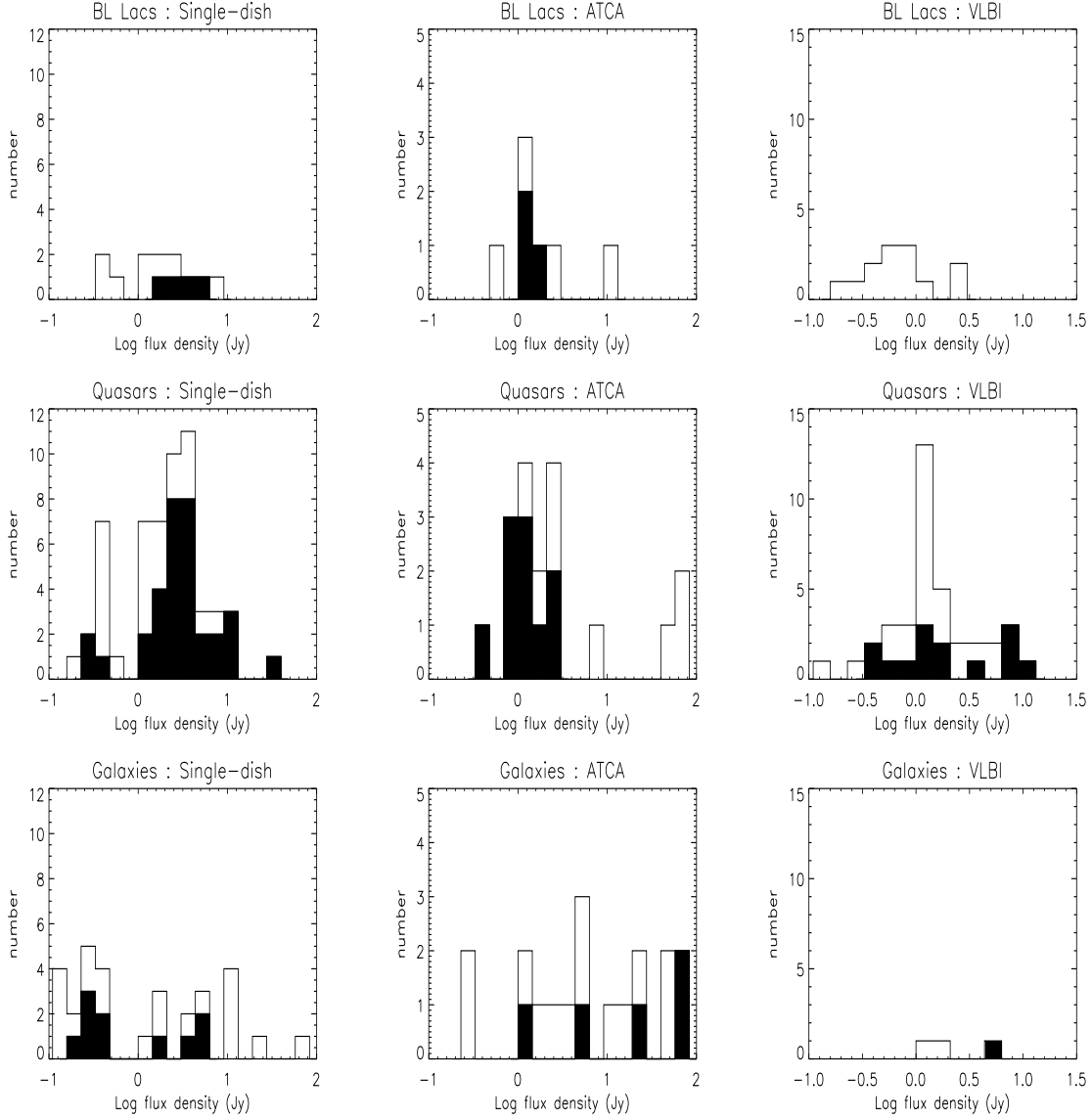


Figure 4. Total intensity VLBI maps of HBLs (a) 1101+384 (b) 1215+303 (c) 1230+253 and (d) 1727+502 at 5 GHz with  $\chi$  vectors superimposed. Contours are (a) -0.17, 0.17, 0.35, 0.70, 1.40, 2.80, 5.70, 11.50, 22.50, 45 and 90 per cent of the peak brightness of  $356 \text{ mJy beam}^{-1}$ ,  $\chi$  vectors:  $1 \text{ mas} = 1.8 \text{ mJy beam}^{-1}$  (b) -0.17, 0.17, 0.35, 0.70, 1.40, 2.80, 5.70, 11.50, 22.50, 45 and 90 per cent of the peak brightness of  $231 \text{ mJy beam}^{-1}$ ,  $\chi$  vectors:  $1 \text{ mas} = 2 \text{ mJy beam}^{-1}$ , (c) -0.17, 0.17, 0.35, 0.70, 1.40, 2.80, 5.60, 11.20, 22.50, 45 and 90 per cent of the peak brightness of  $183 \text{ mJy beam}^{-1}$ ,  $\chi$  vectors:  $1 \text{ mas} = 2.5 \text{ mJy beam}^{-1}$  and (d) -0.35, 0.35, 0.70, 1.40, 2.80, 5.60, 11.20, 22.50, 45 and 90 per cent of the peak brightness of  $64 \text{ mJy beam}^{-1}$ ,  $\chi$  vectors:  $1 \text{ mas} = 1.8 \text{ mJy beam}^{-1}$ .



*Figure 5.* The histograms showing the number of observed and detected (shaded black) BL Lac objects, quasars and radio galaxies with respect to the total flux density, at three different spatial scales for circular polarization (see text for details), with resolution increasing from left to right panels in each row.